Correlated Helix–Coil Transitions in Polypeptides

In past discussions of the growth or decay of a polypeptide α-helix in solution, it has usually been assumed that successive residue transitions occur independently at the helix–coil interface.[1–9] Helix growth or decay has thus been viewed as a Markov process in that the probability that a transition will occur has been assumed not to depend on the elapsed time from the preceding transition.[5] We have been studying helix–coil transitions by computer simulation of the diffusional motions of a model polypeptide[10] and have found that many of the transitions that occur in the simulations are correlated; e.g., the unwinding of a residue is simultaneous with or closely followed by the unwinding of the next residue in the helix. In this note, we consider the nature of correlated helix–coil transitions that occur at the end of a polypeptide chain.

Correlations in the rotational isomeric state transitions of nearby dihedral angles have previously been suggested to play a role in the dynamics of a polymer in solution.[11–16] The physical basis for these suggestions is that in the absence of correlations, rotation about a bond would be opposed by large solvent frictional forces on the rigid portions of the chain connected by the bond. However, the kinds of transitions that occur in a polymer are determined only in part by frictional forces; the forces derived from the effective potential energy also play a role. For alkanes, there is a sizable (~3 kcal/mol) energy barrier for *trans–gauche* isomerization.[17] Strictly concerted transitions (e.g., "crankshaft" motions) are suppressed in such chains because of the large combined activation energy required for such transitions; evidence of significant correlation in the transitions of second-neighbor bonds is apparent in some alkane dynamical simulations[18,19] but not in others.[20] For polypeptides, the intrinsic barriers to rotation about backbone dihedral angles ϕ and ψ are relatively small (~1 kcal/mol),[17,21,22] and the subunit friction coefficients are relatively large, so that correlated transitions might be expected to occur more frequently.

To examine this possibility, we have performed a diffusional dynamics study of the unwinding of two residues at one end of a model polypeptide helix as described in an earlier paper.[10] Neighboring residues are linked by Flory virtual bonds in this model, so that the unwinding can be described using two virtual dihedral angles Φ_1 and Φ_2.[10,17] The effective potential energy surface for the unwinding is shown in Fig. 1(a). The potential well with minimum in region S_1 corresponds to the fully-wound helix. In the rest of the low-energy trough between S_1 and S_2, the terminal residue is in various coil configurations, but the adjacent residue is still in the helix; the minimum in S_2 is the most stable such configuration. For $\Phi_2 \gtrsim 100°$, the two residues at one end of the chain are in coil configurations, but the rest of the chain is helical; the minimum in S_3 is the most stable such configuration. The potential surface includes a discontinuity along the upper boundary of region S_1; for simplicity, this feature is not displayed in Fig. 1(a). The discontinuity prevents motion through the upper boundary, which would correspond to simultaneous rupture of two hydrogen bonds in the helix.[10]

The classical, uncorrelated unwinding of two residues occurs by two successive transitions on the energy surface. The system first moves from the potential well near S_1 to the well near S_2 by crossing the low barrier in the energy trough connecting these wells. After remaining for some time in the S_2 well, the system then moves over a second low barrier to the well in region S_3. In correlated unwinding, the system moves from the S_1 well to the S_3 well without being trapped for a time in S_2. In the present study, a total of 154 diffusional trajectories starting in the S_1 well were observed; the trajectories were terminated upon reaching the surface of region S_2 or S_3. Approximately one out of eight trajectories were of the correlated type; two of these are displayed in Fig. 1(b).

Biopolymers, Vol. 20, 629–632 (1981)

CCC 0006-3525/81/030629-04$01.00

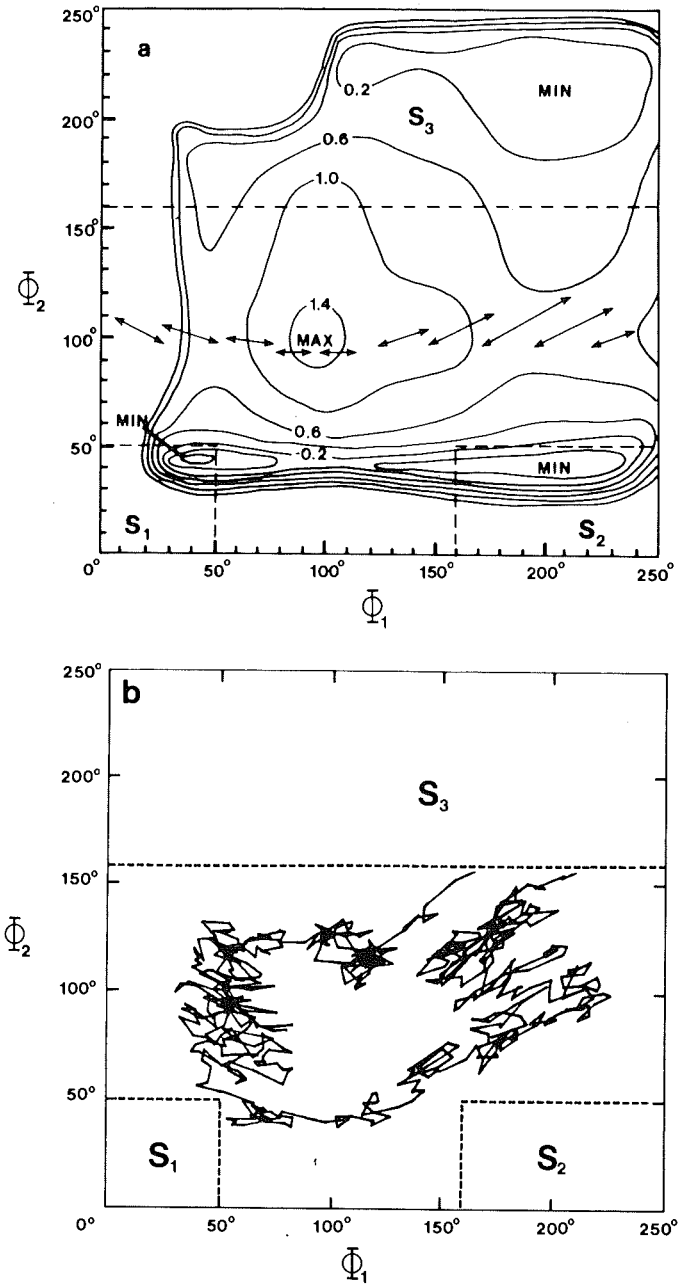

Fig. 1. Configuration space defined by the virtual dihedral angles for the two residues at one end of an α-helical region. (a) The potential of mean force (Ref. 10) with contour intervals of 0.4 kcal/mol. Several contours in the S_1 well are omitted for clarity; the minimum energy in this well is -2.8 kcal/mol. Arrows indicate the preferred directions of diffusion (Ref. 24). (b) Diffusional trajectories for two unwinding motions; the trajectories begin just to the right of region S_1.

The correlated transitions may be understood by considering how the polymer motions are influenced by energy surface and solvent frictional effects. With respect to the latter, it is important to recognize that motion on the energy surface occurs by *anisotropic* diffusion[23,24]; the arrows in Fig. 1(a) represent the preferred directions of diffusional motion on the plane in the absence of any potential-energy variations. These arrows indicate the directions of the eigenvectors with largest eigenvalues of two-dimensional diffusion tensors which are derived elsewhere,[24] but the physical origin of these preferred directions is easily understood. For $\Phi_1 > 90°$, the displacement of the end residue and the attendant viscous dissipation will be minimized during a positive (negative) rotation of Φ_2 if there is a compensating positive (negative) rotation of Φ_1. For $\Phi_1 < 90°$, the dissipation is minimized if Φ_2 and Φ_1 change in opposite fashion. Such anisotropic diffusional effects are the physical basis of the postulated correlations in rotational isomeric state transitions mentioned previously; these effects are expected to govern the polypeptide chain motions in regions where the energy surface is fairly flat and to compete with the forces due to the energy surface in other regions. As described below, these expectations are realized in the polypeptide trajectories.

In the trajectory on the left-hand side of Fig. 1(b), the system moves first along a low-energy trough with increasing Φ_2; although the overall motion is determined by the trough, the anisotropic diffusional effects are clearly evident in the diagonal sideways fluctuations within the trough. The system then moves toward the S_3 minimum along the direction of preferred diffusion and decreasing potential energy. In the trajectory on the right-hand side of Fig. 1(b), the system is forced out of the low-energy trough connecting the S_1 and S_2 minima by the anisotropic frictional effects. A related phenomenon is observed in many of the "classical" trajectories ending in S_2; approximately 40% of these trajectories strayed into the region $\Phi_2 > 70°$ at an energy cost of roughly 2 kcal/mol above the corresponding minimum energy point along the $\Phi_2 = 40°$ pathway.

It is possible that experimental evidence concerning the correlated transitions described here could be obtained from careful measurements of the solvent viscosity dependence of the rate and free energy of activation for helix growth.

This work has been supported in part by grants from the Petroleum Research Fund as administered by the American Chemical Society, the NSF, and the NIH. M.R.P. is an NSF/NRC Postdoctoral Fellow. S.H.N. and R.M.L. are NIH Postdoctoral Fellows. J.A.M. is an Alfred P. Sloan Fellow and the recipient of an NIH Research Career Development Award.

References

1. Schwarz, G. & Engel, J. (1972) *Angew. Chem. Int. Ed.* **11**, 568–575.
2. Tanaka, T., Soda, K. & Wada, A. (1973) *J. Chem. Phys.* **58**, 5707–5715.
3. Miller, W. G. (1973) *Macromolecules* **6**, 100–107.
4. Jernigan, R. L., Ferretti, J. A. & Weiss, G. H. (1973) *Macromolecules* **6**, 684–687.
5. Isbister, D. J. & McQuarrie, D. A. (1974) *J. Chem. Phys.* **60**, 1937–1942.
6. Jernigan, R. L. & Ferretti, J. A. (1975) *J. Chem. Phys.* **62**, 2519–2529.
7. Chay, T. R. & Stevens, C. L. (1975) *Macromolecules* **8**, 531–535.
8. Neves, D. E. & Scott, R. A. (1977) *Macromolecules* **10**, 339–346.
9. Ishiwari, K. & Nakajima, A. (1978) *Macromolecules* **11**, 785–792.
10. McCammon, J. A., Northrup, S. H., Karplus, M. & Levy, R. M. (1980) *Biopolymers* **19**, 2033–2045.
11. Schatzki, T. F. (1965) *Polym. Prepr., Am. Chem. Soc., Div. Polym. Chem.* **6**, 646.
12. Helfand, E. (1971) *J. Chem. Phys.* **54**, 4651–4661.
13. Iwata, K. (1973) *J. Chem. Phys.* **58**, 4184–4202.
14. Blomberg, C. (1979) *Chem. Phys.* **37**, 219–227.

15. Morawetz, H. (1980) *Pure Appl. Chem.* **52,** 277–284.
16. Pear, M. R. & Weiner, J. H. (1980) *J. Chem. Phys.* **72,** 3939–3947.
17. Flory, P. J. (1969) *Statistical Mechanics of Chain Molecules,* Wiley, New York.
18. Helfand, E., Wasserman, Z. R. & Weber, T. A. (1979) *J. Chem. Phys.* **70,** 2016–2017.
19. Helfand, E., Wasserman, Z. R. & Weber, T. A. (1980) *Macromolecules* **13,** 526–533.
20. Montgomery, J. A., Holmgren, S. L. & Chandler, D. (1980) *J. Chem. Phys.* **73,** 3688–3694.
21. Tsuji, Y., Yasunaga, T., Sano, T. & Ushio, H. (1976) *J. Am. Chem. Soc.* **98,** 813–818.
22. Gruenewald, B., Nicola, C. U., Lustig, A., Schwarz, G. & Klump, H. (1979) *Biophys. Chem.* **9,** 137–147.
23. Knauss, D. C. & Evans, G. T. (1980) *J. Chem. Phys.* **72,** 1504–1511.
24. Pear, M. R., Northrup, S. H. & McCammon, J. A. (1980) *J. Chem. Phys.* **73,** 4703–4704.

MICHAEL R. PEAR
SCOTT H. NORTHRUP*
J. ANDREW MCCAMMON

Department of Chemistry
University of Houston
Houston, Texas 77004

MARTIN KARPLUS
RONALD M. LEVY†

Department of Chemistry
Harvard University
Cambridge, Massachusetts 02138

Received July 25, 1980
Accepted November 4, 1980

* Present address: Department of Chemistry, Tennessee Technological University, Cookeville, Tennessee 38501.
† Present address: Department of Chemistry, Douglass College, Rutgers University, New Brunswick, New Jersey 08903.